PCCP

PAPER

View Article Online
View Journal | View Issue



Cite this: *Phys. Chem. Chem. Phys.*, 2017, **19**, 11340

# Kinetics of crystalline nuclei growth in glassy systems

Anatolii V. Mokshin *[ab] and Bulat N. Galimzyanov [ab]

In this work, we study crystalline nuclei growth in glassy systems, focusing primarily on the early stages of the process, during which the size of a growing nucleus is still comparable with the critical size. On the basis of molecular dynamics simulation results obtained for two crystallizing glassy systems, we evaluate the growth laws of the crystalline nuclei and the parameters of the growth kinetics at temperatures corresponding to deep supercooling; herein, a statistical treatment of the simulation results is carried out using the mean-first-passage-time method. It is found that for the considered systems at different temperatures, the crystal growth laws that were rescaled onto the waiting times of the critically-sized nuclei follow a unified dependence, and can significantly simplify the theoretical description of the post-nucleation growth of crystalline nuclei. The evaluated size-dependent growth rates are characterized by a transition to the steady-state growth regime, which depends on the temperature and occurs in the glassy systems when the size of a growing nucleus becomes two-three times larger than the critical size. It is suggested that the temperature dependencies of the crystal growth rate characteristics should be considered by using the reduced temperature scale $\tilde{T}$. Thus, it is revealed that the scaled values of the crystal growth rate characteristics (namely, the steady-state growth rate and the attachment rate for the critically-sized nucleus) as functions of the reduced temperature $\tilde{T}$ for glassy systems follow unified power-law dependencies. This finding is supported by the available simulation results; the correspondence with the experimental data for the crystal growth rates in glassy systems at temperatures near the glass transition is also discussed.

Received 9th February 2017,
Accepted 27th March 2017

DOI: 10.1039/c7cp00879a

rsc.li/pccp



## 1 Introduction

A first-order phase transition starts with the formation of the nuclei of a new phase. In particular, nascent liquid droplets represent the nuclei of the new (liquid) phase in the case of vapor condensation. Moreover, vapor bubbles are the nuclei in the case of liquid evaporation, while crystallization is initiated through the formation of crystalline nuclei. According to the classical point of view,[1–5] the nucleus of a new phase is capable of demonstrating steady growth when it reaches a critical size (see Fig. 1). The initial stage of nucleus growth proceeds through the attachment of particles of the parent phase to the nucleus. When the concentration of the growing nuclei becomes high enough, this growth regime is replaced by growth through the coalescence of adjacent growing nuclei. The corresponding three processes, nucleation, growth by attachment of particles and growth through coalescence of growing nuclei, represent the general basis of any first-order phase transition,[1] whilst the

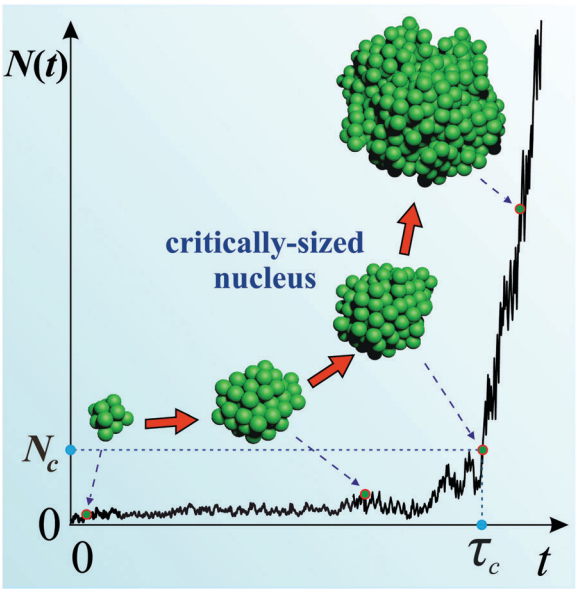


Fig. 1 Schematic of the growth trajectory of the largest crystalline nucleus in a system. Stable growth of a nucleus is possible when a nucleus reaches the critical size, $N_c$. Here, $\tau_c$ is the waiting nucleation time.

[a] *Institute of Physics, Kazan Federal University, 420008 Kazan, Russia. E-mail: anatolii.mokshin@mail.ru*
[b] *L. D. Landau Institute for Theoretical Physics, Russian Academy of Sciences, 117940 Moscow, Russia*

characteristic time scales and rates of the processes are determined by the thermodynamic conditions as well as by the inherent features of a system, mainly, the type of interaction between the structural elements (*e.g.* particles) that form a system.

If we restrict our consideration to the crystallization kinetics of supercooled liquids, then it is possible for this case to distinguish the inherent features. Upon increasing the supercooling level, which can be quantified by $\Delta T/T_m$, where $T_m$ is the melting temperature and $\Delta T = T_m - T$, the crystal nucleation driving force increases and, thereby, accelerates structural ordering in the supercooled liquid. Furthermore, upon further increase in the supercooling level, structural transformations slow down due to the increased viscosity. At a supercooling level that is high enough to correspond to the glass transition temperature $T_g$, the viscosity of a supercooled liquid becomes $\eta \simeq 10^{12}$ Pa s. As a consequence of the high viscosity, the structural transformations in the glass occur so slowly that the overall crystallization of the glass at a temperature of $T \ll T_g$ is almost unobservable over an acceptable time scale, albeit the separate crystal nucleation events still occur.[6] Moreover, the extremely small sizes and low concentrations of nascent crystalline nuclei as well as the very low rates of crystal nucleation and crystal growth complicate studies of the initial regimes of crystallization in glasses by conventional experimental methods. Therefore, even if the growth of crystalline clusters in supercooled fluids at low and moderate levels of metastability is a sufficiently well-studied subject, there are still many disputed issues relating to structural ordering in glasses.[2,7–13] Remarkably, techniques based on molecular dynamics simulations appear to be fruitful for elucidating the microscopic mechanisms of the initial stages of nucleation and growth processes for such thermodynamic conditions where experimental methods encounter difficulties.[1,14–19]

In a recent paper,[20] it was reported that the structural ordering in two model glassy systems proceeds through the nucleation mechanism. For both systems, the nucleation times evaluated as functions of temperature followed the unified scaling law, which was also confirmed by experimental data for the stoichiometric glasses near the glass transition. In the present study, we extend the results of ref. 20 to a consideration of the growth kinetics of crystalline nuclei in glassy systems by focusing mainly on the initial stage of crystalline nuclei growth, in which the non-stationary effects associated with nucleus size fluctuations and the strong size- and time-dependencies of the nucleus growth rate can be very significant. In this study, we apply a statistical treatment of the simulation results for the growth kinetics, that is realized within the suggested method of inverted averaging of the independent growth trajectories. As a result, a growth law, with the characteristics of growth rate, growth lag-time and growth exponent, is defined for each considered thermodynamic state of the system, and a corresponding theoretical description becomes possible. Since the growth trajectories are monitored directly starting from a nucleation event, then both the non-stationary and steady-state growth regimes are accessible for analysis. In addition, the temperature dependencies of the evaluated rate characteristics of crystal growth kinetics as well as their correspondence to the known experimental data are discussed.

# 2 Nuclei growth

## 2.1 General definitions

Let us start with the growth rate of a nucleus, with a size that overcomes the critical value. This quantity can be expressed in terms of the number of particles $N$ as

$$\upsilon_N = \frac{dN}{dt} \tag{1a}$$

and through the average radius $R$ as

$$\upsilon_R = \frac{dR}{dt}. \tag{1b}$$

Both of the quantities $\upsilon_N$ and $\upsilon_R$ are positive when the cluster has a size larger than the critical size, *i.e.* $N > N_c$ and $R > R_c$. Here, $N_c$ is the critical value of the number of particles that form the nucleus, and $R_c$ is the critical value of the nucleus radius. Within the notations of the Becker–Döring gain-loss theory for nucleation, the growth rate $\upsilon_N$ is defined as the difference between the attachment-rate $g^+(N)$ and detachment-rate $g^-(N)$ coefficients, *i.e.*[21]

$$\upsilon_N = g^+(N) - g^-(N). \tag{2}$$

Taking into account the detailed balance condition

$$g^+(N-1)P(N-1) = g^-(N)P(N), \tag{3a}$$

where

$$P(N) = P_0 \exp\left(-\frac{\Delta G(N)}{k_B T}\right) \tag{3b}$$

is an equilibrium cluster distribution, one obtains

$$\upsilon_N = g^+(N) - g^+(N-1)\exp\left[-\frac{\Delta G(N-1) - \Delta G(N)}{k_B T}\right], \tag{4}$$

which is known as the growth equation of the Becker–Döring gain-loss theory.[21] Here, $\Delta G(N)$ is the free energy cost required to form a nucleus of size $N$, $k_B$ denotes the Boltzmann constant, $T$ is the absolute temperature and $P_0$ is a pre-exponential factor. The continuous version of this equation has the form[22]

$$\upsilon_N = g^+(N)\left\{1 - \exp\left[\frac{1}{k_B T}\frac{d\Delta G(N)}{dN}\right]\right\} + \frac{dg^+(N)}{dN}\exp\left[\frac{1}{k_B T}\frac{d\Delta G(N)}{dN}\right]. \tag{5}$$

Moreover, according to classical nucleation theory, the free energy, $\Delta G(N)$, represents the sum of the negative bulk contribution $-|\Delta\mu|N$ and the positive surface contribution $\alpha_s N^{2/3}$, *i.e.*

$$\Delta G(N) = -|\Delta\mu|N + \alpha_s N^{2/3}, \tag{6}$$

where $|\Delta\mu|$ is the difference between the chemical potential per phase unit of the melt and the crystal, and $\alpha_s$ is the temperature-dependent coefficient which is proportional to the interfacial free energy $\gamma_s$. For the spherical cluster one has

$\alpha_s = (36\pi)^{1/3}\gamma_s/\rho_c^{2/3}$, with $\rho_c$ being the numerical density of the nascent (crystalline) phase. From eqn (6) one finds

$$\frac{d\Delta G(N)}{dN} = |\Delta\mu|\left[\left(\frac{N_c}{N}\right)^{1/3} - 1\right], \tag{7}$$

where

$$N_c = \left(\frac{2}{3}\frac{\alpha_s}{|\Delta\mu|}\right)^3 \tag{8}$$

is the critical cluster size. By inserting eqn (7) into eqn (5), one obtains

$$\begin{aligned} \upsilon_N = g^+(N)\left\{1 - \exp\left[\frac{|\Delta\mu|}{k_B T}\left(\left(\frac{N_c}{N}\right)^{1/3} - 1\right)\right]\right\} \\ + \frac{dg^+(N)}{dN}\exp\left[\frac{|\Delta\mu|}{k_B T}\left(\left(\frac{N_c}{N}\right)^{1/3} - 1\right)\right]. \end{aligned} \tag{9}$$

Note that relation (9) has a clear physical meaning. Namely, it indicates that the growth rate, $\upsilon_N$, corresponds to the kinetic rate, $g^+(N)$, which is weighted by a thermodynamic factor, the term in curly brackets, which represents the fraction of added particles that is not removed due to the detachment process. Hence, eqn (4), (5) and (9) define the growth rate, $\upsilon_N$, of a nucleus with a size that is larger than the critical size, $N_c$, and validity of equations is not restricted by specific shape of a nucleus or by a supercooling range. At the same time, it might be useful to consider some conditions that lead to known results and models for the growth rate[23] (in the appendix, see the Zeldovich relation (23) for the growth rate, the Wilson–Frenkel theory with eqn (25) and (29), the Turnbull–Fisher model with a general relation (33) and the Kelton–Greer extension with eqn (35) and (39)). In particular, in the case of weak size-dependence on the attachment rate, growth eqn (9) takes the form

$$\upsilon_N = g^+(N)\left\{1 - \exp\left[\frac{|\Delta\mu|}{k_B T}\left(\left(\frac{N_c}{N}\right)^{1/3} - 1\right)\right]\right\} \tag{10}$$

which usually represents a basis for various growth models.[1]

### 2.2 Growth of nuclei with near-critical sizes

Taking into account eqn (9) and the attachment rate of a generally accepted form [see eqn (43) in Appendix]:

$$g^+(N) = g^+(N_c)\left(\frac{N}{N_c}\right)^{(3-p)/3}, \quad 0 < p \le 3, \tag{11}$$

one can directly obtain

$$\begin{aligned} \upsilon_N = \frac{dN}{dt} = g^+_{N_c}\left(\frac{N}{N_c}\right)^{\frac{3-p}{3}} \\ \times\left\{1 + \left(\frac{3-p}{3N} - 1\right)\exp\left[\frac{|\Delta\mu|}{k_B T}\left(\left(\frac{N_c}{N}\right)^{1/3} - 1\right)\right]\right\}, \\ 0 < p \le 3. \end{aligned} \tag{12}$$

It is important to stress that eqn (12) follows directly on from equation (2) for the growth rate and that no additional conditions were applied to the values of the critical size and to the metastability level as is done in the cases of *ad hoc* growth models. This equation as well as the continuity equation for the evolving size distribution of the nuclei and the law of conservation of matter form the set of equations that is necessary to be resolved in order to reproduce the kinetics of an arbitrary realistic first-order phase transition.[24] Here, $g^+(N_c)$ is the attachment rate for the critically-sized nucleus. As is known, the exponent, $p$, takes integer values for well-defined growth models including the ballistic and diffusion-limited models (the corresponding discussion of this issue can be found in ref. 23). If the exponent $p = 3$, then the attachment rate is independent of the nucleus size. For other limiting cases where $p = 0$, the attachment rate changes with increasing nucleus size according to $g^+(N) \sim N$. Mixed growth regimes can also arise with non-integer values of the parameter $p$.[25,26] This is seen in the kinetic growth models (41)–(43) given in the appendix. In particular, it is quite reasonable to expect that non-integer values of the parameter $p$ will correspond to the growth of nuclei with near-critical sizes, since there is no clearly defined regime of growth at such sizes, while stochastic effects in post-nucleation growth are significant. Finding the general growth law, $N(t)$, that is an exact solution of eqn (12) and which will be valid for a whole size domain and for different growth regimes, is a difficult task. Instead of directly resolving the differential of eqn (12), we apply other method. Namely, the growth law of nuclei of near-critical sizes can be formally defined by the corresponding Taylor series expansion:

$$\begin{aligned} N(t) = N_c + \left.\frac{dN(t)}{dt}\right|_{t\approx\tau_c}(t-\tau_c) + \frac{1}{2}\left.\frac{d^2N(t)}{dt^2}\right|_{t\approx\tau_c}(t-\tau_c)^2 \\ + \frac{1}{6}\left.\frac{d^3N(t)}{dt^3}\right|_{t\approx\tau_c}(t-\tau_c)^3 + \mathcal{O}\left(|t-\tau_c|^4\right). \end{aligned} \tag{13}$$

Then, from eqn (11) and (12) one finds that expansion (13) can be approximated in the following way:

$$N(t) = N_c + \sum_{k=1}^{3} A_k (t-\tau_c)^k, \tag{14a}$$

with the coefficient

$$\begin{aligned} A_k \simeq \frac{3-p}{3N_c k!}\left(g^+_{N_c}\right)^k\left(\frac{\beta|\Delta\mu|}{3N_c}\right)^{k-1}, \\ 0 < p \le 3, \end{aligned} \tag{14b}$$

where $g^+_{N_c} \equiv g^+(N_c)$ and $\beta = 1/(k_B T)$. As can be seen from eqn (14), the nucleus growth, as defined by eqn (14), is represented by the sum of three contributions, according to which the nucleus size $N(t)$ evolves as a function of the sum of $\sim t$, $\sim t^2$ and $\sim t^3$. The coefficient $A_1 = (3-p)g^+_{N_c}\big/3N_c$ is the growth factor, which has dimensions of inverse time and corresponds to the effective growth rate in the initial growth regime, *i.e.* $A_1 \equiv \theta_c$. Furthermore, the coefficient $A_2$ accounts for the growth acceleration effects, whereas the term $A_3$ quantifies the change in the growth

 

acceleration over time for nuclei of near-critical sizes. By using eqn (14) and the known quantities $\tau_c$ and $N_c$, one can evaluate the attachment rate $g_{N_c}^{+}$, the reduced chemical potential difference $\beta|\Delta\mu|$ and the growth exponent $p$ by fitting eqn (14) to an "experimentally" measured growth law.

## 3 Simulation details

We consider the growth of crystalline nuclei in two different glass-formers: the single-component Dzugutov (Dz) system with the potential[27]

$$\frac{U_{\mathrm{Dz}}(r^*)}{\varepsilon} = C(r^{*-m} - D)\exp\left(\frac{c}{r^* - a}\right)\Theta(a - r^*) + D\exp\left(\frac{d}{r^* - b}\right)\Theta(b - r^*), \qquad r^* = r_{ij}/\sigma \tag{15}$$

and the binary Lennard-Jones (bLJ) system $A_{80}B_{20}$, where the particles interact *via* the potential[20]

$$\frac{U_{\mathrm{bLJ}}\left(r_{\alpha\beta}{}^*\right)}{\varepsilon_{\alpha\beta}} = 4\left[\left(r_{\alpha\beta}{}^*\right)^{-12} - \left(r_{\alpha\beta}{}^*\right)^{-6}\right], \qquad r_{\alpha\beta}{}^* = r_{ij}^{\alpha\beta}/\sigma_{\alpha\beta}, \qquad \alpha,\beta \in \{\mathrm{A},\mathrm{B}\} \tag{16}$$

The numerical values of the parameters for both of the potentials are presented in Table 1. Here, $r_{ij}$ is the distance between the $i$-th and $j$-th particles, and $\Theta(\cdots)$ is the Heaviside step-function. In the case of the bLJ-system with the potential shown in (16), the labels A and B denote the type of particle, and the semi-empirical (incomplete) Lorentz–Berthelot mixing rules are applied (see Table 1). The characteristics of the potentials $\sigma$ and $\varepsilon$ correspond to the unit distance and unit energy, respectively, whilst the unit time is $\tau = \sigma\sqrt{m/\varepsilon}$; the particles are of the same mass, *i.e.* $m = m_A = m_B = 1$.† [20]

Simulations with the time step $\Delta t = 0.005\tau$ were performed in the $\mathcal{N}PT$-ensemble, where the temperature, $T$, and pressure, $P$, were controlled using a Nosé–Hoover thermostat and barostat.[20] For a single simulation run, $\mathcal{N} = 6912$ particles were included in a cubic simulation cell with the volume $V = l_x{}^3$, $l_x = l_y = l_z \simeq 20\sigma$, and periodic boundary conditions were imposed onto all of the directions. Glassy samples were generated by fast isobaric cooling with the rate $\mathrm{d}T/\mathrm{d}t = 0.001\varepsilon/(k_B\tau)$ of a well equilibrated fluid according to the algorithm presented in detail in ref. 20. As a result, glassy samples were prepared at temperatures below the glass-transition temperature $T_g$ along the isobars with pressure $P = 14\varepsilon/\sigma^3$ for the Dz-system and with pressure $P = 17\varepsilon/\sigma^3$ for the bLJ-system. The Dz-system at pressure $P = 14\varepsilon/\sigma^3$ is characterized by a melting temperature of $T_m \simeq 1.51\varepsilon/k_B$ and a glass transition temperature of $T_g \simeq 0.65\varepsilon/k_B$ at such a cooling rate,[28] while the bLJ-system at pressure $P = 17\varepsilon/\sigma^3$ is characterized by a melting temperature of $T_m \simeq 1.65\varepsilon/k_B$ and a glass transition temperature of $T_g \simeq 0.92\varepsilon/k_B$.

Note that to perform the statistical treatment of the simulation results, more than fifty independent samples were generated for each considered $(P,T)$-state of the systems.

Table 1 Parameters of the Dz-potential (15) and bLJ-potential (16)

| Dz | | | | | | |
|---|---|---|---|---|---|---|
| $C$ | $D$ | $m$ | $a$ | $b$ | $c$ | $d$ |
| 5.82 | 1.28 | 16 | 1.87 | 1.94 | 1.1 | 0.27 |
| bLJ | | | | | | |
| $\sigma_{\alpha\alpha}$ | $\varepsilon_{\alpha\alpha}$ | $\sigma_{\beta\beta}$ | $\varepsilon_{\beta\beta}$ | $\sigma_{\alpha\beta}$ | $\varepsilon_{\alpha\beta}$ | |
| $1.0\sigma$ | $1.0\varepsilon$ | $0.8\sigma$ | $0.5\varepsilon$ | $0.9\sigma$ | $1.5\varepsilon$ | |

† Note that the binary Lennard-Jones system considered here is characterized by different mixing rules in comparison with the Kob-Anderson and Wahnström binary Lennard-Jones systems. Thereby, it differs from these systems, which form very stable glassy states and which do not crystallize over simulation time scales.

## 4 Nucleation parameters and growth curves from molecular dynamics simulation data

Classical molecular dynamics simulations allow one to obtain information about the positions of all of the particles that generate the system. In order to identify the nuclei of an ordered phase for an instantaneous configuration of the system we apply the cluster analysis that was introduced originally in ref. 29 and based upon computation of the local orientational order parameters, $q_4(i)$, $q_6(i)$ and $q_8(i)$, for each $i$th particle.[30] Details of the algorithm are given in ref. 20 and 31. By means of cluster analysis we obtain, for each $\alpha$th simulation run, the time-dependent growth trajectory $N_\alpha(t)$, which defines the number of particles that belong to the largest nucleus in the system at time $t$. Here, $\alpha$ is the label of the simulation run for the $(P,T)$-state. Four growth trajectories, $N(t)$, of the largest nucleus from the independent molecular dynamics simulations are shown in Fig. 2(a). Moreover, from the set of trajectories, $N_\alpha(t)$, where $\alpha = 1, 2, 3, \ldots, 50$, for the $(P,T)$-state, the curve $\bar{t}(N)$ is defined, which is known as the mean-first-passage-time curve and which characterizes the average time of the first appearance of a nucleus with a given size, $N$. In accordance with the mean-first-passage-time method,[32] the inflection point of this curve gives the critical size, $N_c$, and the average time, $\tau_c$, that are needed to reach it, *i.e.* $\tau_c \equiv \bar{t}(N_c)$. As an example, Fig. 2(c) shows a typical mean-first-passage-time curve that is derived from growth trajectories including those shown in Fig. 2(a). Furthermore, the inverted mean-first-passage-time curve $N(\bar{t})$ for sizes $N \geq N_c$ and times $t \geq \tau_c$ will reproduce the growth law of a nucleus in a system [see Fig. 2(b)]. Then, the curve, $N(\bar{t})$, can be used to extract the values of the growth parameters or to test a theoretical model of nucleus growth.[33]

The attachment rate $g_{N_c}^{+}$ can be computed on the basis of the molecular dynamics simulation data by means of the method

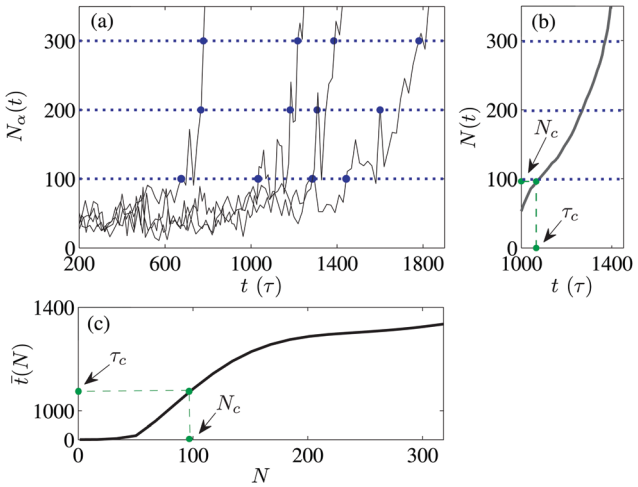


Fig. 2 Statistical treatment of the simulation results within the mean-first-passage-time method. (a) Time-dependent growth trajectories $N_\alpha(t)$ of the largest nucleus extracted from the data of four independent simulation runs ($\alpha$ = 1, 2, 3 and 4) for the system in the ($P$,$T$)-state. (b) Growth law, $N(t)$, of the largest nucleus recovered by averaging over fifty growth trajectories including the four shown in (a). (c) Mean-first-passage-time curve defined for the size of the largest nucleus. The inflection point of this curve defines the critical size, $N_c$, and the average waiting time of the critically-sized nucleus, $\tau_c \equiv \bar{t}(N_c)$.

suggested in ref. 29. Namely, the quantity $g^+_{N_c}$ is defined by the mean-square change of the nucleus size in the vicinity of the critical size:

$$g^+_{N_c} = \frac{\left\langle [N(t) - N_c]^2 \right\rangle}{2\tau_w}, \qquad (17)$$

where $t \in [\tau_c - \tau_w; \tau_c + \tau_w]$ and $\tau_w$ is the time window over which the nucleus evolution is traced.‡ The angle brackets $\langle \cdots \rangle$ correspond to the average over independent growth trajectories, $N(t)$.

# 5 Results

## 5.1 Growth laws

Cluster analysis reveals that the particles of the growing clusters mainly correspond to the fcc structure, while the low amount of surface particles corresponds to an hcp structure. This is observed for both of the systems at all of the considered temperatures. Fig. 3 demonstrates, as an example, the crystalline clusters that emerge in the Dz- and bLJ-systems and which are recognized by means of cluster analysis.

The growth curves of the first (largest) crystalline nucleus in the glassy Dz- and bLJ-systems at different temperatures are presented in Fig. 4 (top panel). Here, the results correspond to the earliest stage of nucleus growth, during which the nucleus size increases threefold. As was expected, the growth process slows down with decreasing temperature, $T$. This is evidenced for both of the systems by a shift of the growth curves at lower temperatures to domains of longer times.

‡ In this work, the computation of $g^+_{N_c}$ was carried out using the data obtained for the largest crystalline nucleus.

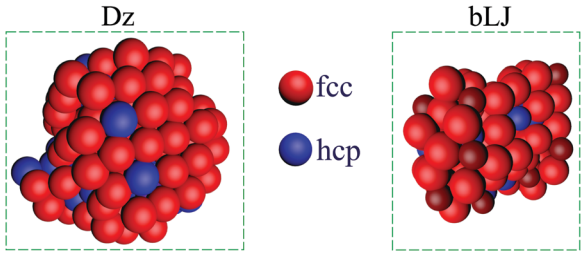


Fig. 3 Snapshots of the crystalline clusters arising in the Dz-system at $T$ = $0.5\varepsilon/k_B$ and in the bLJ-system at $T$ = $0.3\varepsilon/k_B$, with the particles recognized as belonging to the fcc and hcp crystalline phases.

In the middle panel of Fig. 4, the growth curves are shown in a rescaled form, according to which the time-scale is expressed in units of the waiting time, $\tau_c$. Moreover, units are subtracted from the times in the rescaling in order to relate the start of nucleus growth to the zeroth time. As a result of the rescaling, the growth curves collapse onto a master-curve. The unified behavior of the rescaled growth curves with respect to the temperature, $T$, which is observed in Fig. 4, indicates that the crystal nucleation and growth processes in the glassy systems could be of the same kinetic origin. This means that there are unified growth kinetics mechanisms in the glassy systems, and that the corresponding theoretical description could be obtained within a general kinetic model for the growth law. We note that similar features were observed before for the growth of crystalline nuclei in a model glassy system under homogeneous shear[34–37] as well as for droplet growth in supersaturated water vapor.[33]

Taking into account that for each of the considered ($P$,$T$)-states of both of the systems, the attachment rate $g^+(N_c)$ is determined (this will be discussed below), while the critical size, $N_c$, as well as the waiting time, $\tau_c$, are computed by means of the mean-first-passage-time method,[20] it becomes possible to fulfil the fitting of the growth curves presented in Fig. 4 (middle panel) by eqn (14) by using the reduced chemical potential difference $\beta|\Delta\mu|$ and the growth exponent $p$ as adjustable parameters.§ The values of the nucleation characteristics (the critical size, $N_c$, and the average waiting time of the critically-sized nucleus, $\tau_c$), determined by means of the method presented in Section 4 on the basis of fifty independent trajectories $N_\alpha(t)$ for each temperature, are given in Table 2. As can be seen from Fig. 4 (bottom panel), the resultant master-curves of the crystalline nuclei growth in both of the systems are reproducible by the growth law (14). Consider that the presented growth curves are a result of averaging over fifty independent growth trajectories. As demonstrated in our analysis, such statistics are not sufficient to obtain a perfect collapse for all of the cases over the whole considered time range. Nevertheless, this is quite enough to observe the unified behavior of the growth curves, as seen in the results of Fig. 4. Insignificant deviations of the master-curves from the growth law (14) are

§ As shown previously in ref. 38 and 39, all of the particles of a binary system can be considered without division into subtypes with relatively small differences in the characteristics of a binary system such as partial concentrations, particle masses and particle sizes.

 

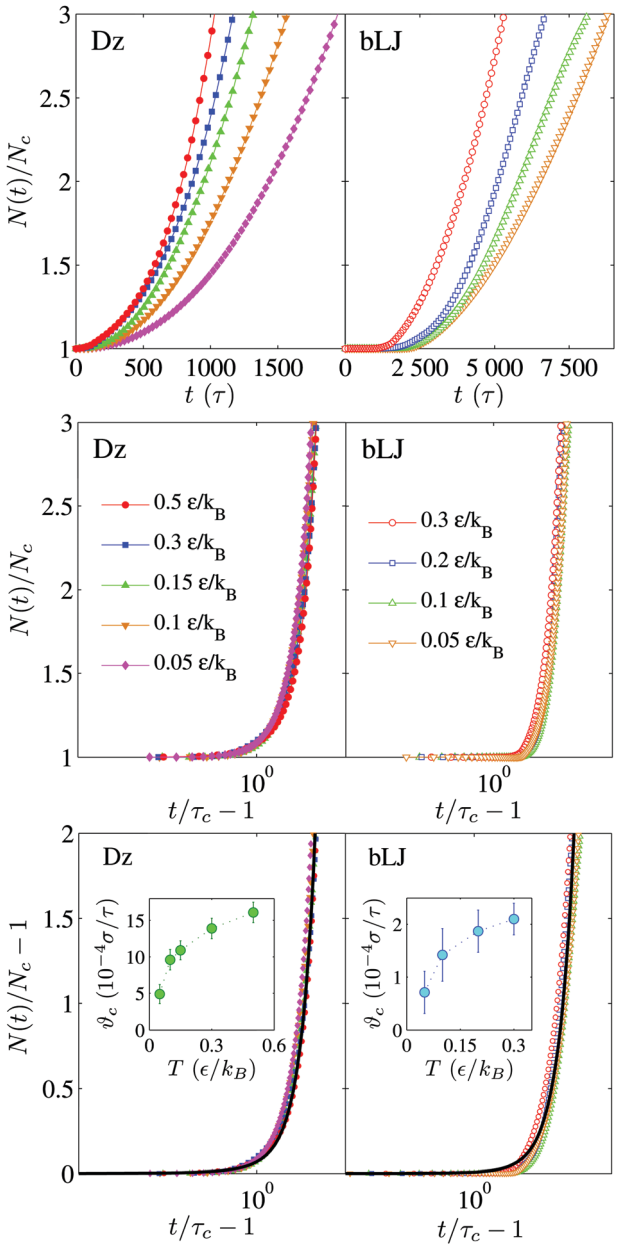


Fig. 4 Top panel: Growth curves of the largest crystalline nucleus in the glassy Dz- and bLJ-systems at different temperatures. Each growth curve is a result of the statistical averaging of the evolution trajectories for the largest nucleus, as evaluated from the independent simulation runs. For clarity, the nucleus size, $N(t)$, is rescaled onto the critical size, $N_c$. Middle panel: Growth curves rescaled onto the waiting time of the critically sized nucleus, $\tau_c$. For clarity, the time-axis is presented on a logarithmic scale. Bottom panel: (main) Rescaled growth curves fitted by eqn (14). The dotted curves correspond to the simulation results; the solid curves represent the fit of eqn (14). Inset images: Temperature dependencies of the evaluated growth factor $\theta_c$.

completely covered by small numerical errors of the estimated values of the quantities $\beta|\Delta\mu|$ and $p$. We found that the growth exponent $p$ takes the value $p = 2.8 \pm 0.15$ for the Dz-system and $p = 2.99 \pm 0.01$ for the bLJ-system. Note that the values of the exponent $p$ do not change for both of the systems over the whole of the considered temperature range. The growth laws

Table 2 Values of the critical size, $N_c$, and the average waiting time of the critically-sized nucleus, $\tau_c$

| | $T\ (\varepsilon/k_B)$ | $N_c$ | $\tau_c\ (\tau)$ |
|---|---|---|---|
| Dz | 0.05 | 88 ± 6 | 372 ± 60 |
| | 0.1 | 92 ± 5 | 340 ± 55 |
| | 0.15 | 96 ± 5 | 305 ± 40 |
| | 0.3 | 105 ± 6 | 250 ± 40 |
| | 0.5 | 108 ± 5 | 220 ± 30 |
| bLJ | 0.05 | 55 ± 3 | 820 ± 80 |
| | 0.1 | 57 ± 4 | 800 ± 75 |
| | 0.2 | 58 ± 4 | 795 ± 65 |
| | 0.3 | 59 ± 4 | 785 ± 60 |

with these exponent values indicate that the attachment rate is practically independent of the nucleus size, $g^+(N) \simeq g^+_{N_c}$, at the earliest stage of nucleus growth. Note that deviation of the values of parameter $p$ from integers can be due to the fact that there is no clearly defined regime of nucleus growth at such sizes, while stochastic effects during post-nucleation growth are significant. Furthermore, we find that the reduced chemical potential $\beta|\Delta\mu|$ is practically unchanged for the systems within the considered temperature range. Values of $\beta|\Delta\mu| = 0.215 \pm 0.016$ and $0.167 \pm 0.014$ over the temperature range of $[0.05; 0.5]\varepsilon/k_B$ are observed in the case of the Dz-system, and values of $\beta|\Delta\mu| = 0.131 \pm 0.013$ and $0.122 \pm 0.013$ over the temperature range of $[0.05; 0.3]\varepsilon/k_B$ are observed in the case of the bLJ-system.

### 5.2 Growth rate

As seen in Fig. 4, some time after nucleus growth has started, the steady growth regime is established, whereby the time-dependent nucleus size is well interpolated by a linear dependence. Since the time derivative of a growth curve defines the time-dependent growth rate $\upsilon(t)$ [according to definition (1a)], then the derivative has to approach a constant value, $\upsilon^{(st)}$, for the steady-state growth regime.¶ The growth rate as function of time, $\upsilon(t)$, was numerically computed for each of the considered states of the systems on the basis of the growth trajectories, $N(t)$, and the size-dependent growth rate, $\upsilon_N$, was determined from the available data for $N(t)$ and $\upsilon(t)$ by simple correspondence of the rates, $\upsilon$, and nucleus sizes, $N$, at the same time points.

The computed growth rates as functions of the rescaled sizes, $N/N_c$, of the systems at different temperatures are shown in Fig. 5. As is expected, the lower growth rates correspond to the states at lower temperatures. One can see from the figure that the growth rate, $\upsilon_N$, increases initially with the size, $N$, and then reaches a steady-state value, $\upsilon^{(st)}$, for each considered case. Remarkably, the steady-state growth regime occurs when the cluster size is still comparable with the critical size $N_c$. For the glassy Dz-system at temperatures of $T = [0.05; 0.5]\varepsilon/k_B$, the transition into steady-state growth occurs at a cluster size of $N \simeq [2.5; 3]N_c$, whereas for the glassy bLJ-system at temperatures of $T = [0.05; 0.3]\varepsilon/k_B$, the transition occurs at $N \simeq [1.7; 3]N_c$.

¶ Note that the steady-state growth regime here means a case in which the growth rate becomes independent of time.

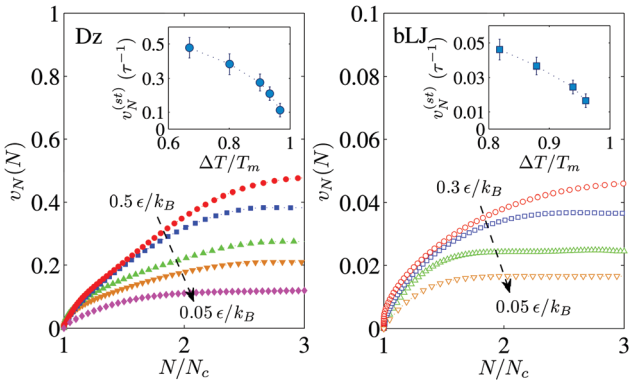


Fig. 5 Main panels: Growth rate curves, $\upsilon_N$, dependent on the crystalline nucleus size for the Dz- and bLJ-systems at different temperatures. Inset images: Steady-state growth rate, $\upsilon_N^{(st)}$, as a function of $\Delta T/T_m$. Note that the growth law, eqn (13), and its time derivative, $dN(t)/dt$, represent the parametric equations for $\upsilon_N(N)$. The values of the steady-state growth rate, $\upsilon_N^{(st)}$, were estimated by means of numerical solution of the parametric equations.

Moreover, the lower the temperature, $T$, the smaller the value of the cluster size at which the transition occurs.

The steady-state growth rate, $\upsilon_N^{(st)}$, *vs.* the supercooling level, $\Delta T/T_m$, is shown in the inset images in Fig. 5. As can be seen, the growth rates, $\upsilon_N^{(st)}$, for both of the systems decrease with increasing supercooling, $\Delta T/T_m$, in such a way that the growth rates are extrapolated to the zeroth values as we approach $\Delta T/T_m = 1$ and $T_0 = 0$ K. The observed temperature dependence of the steady-state growth rate, $\upsilon_N^{(st)}$, differs from that which appears at low levels of supercooling, where the growth rate, $\upsilon_N^{(st)}$, is proportional to $\Delta T/T_m$ [see eqn (28), (29) and (40) in the appendix].

As can be seen in the inset images in Fig. 5, the temperature dependencies of the steady-state growth rates for both of the systems are similar. If such a behavior is a common physical origin for levels of supercooling, then the behavior has to be reproducible within a unified scaling relation, in which the scaled values of the rate characteristic (and the growth rate) should be taken as a function of the reduced temperature.[20] For the temperature range of $0 < T < T_m$ corresponding to a supercooled liquid and glass, it seems to be natural to use $T/T_m$ or the supercooling temperature, $(T_m - T)/T_m$, as the reduced temperature. However, in this case, a reasonable consistency in the scaling can be expected only at temperatures near the melting temperature.[6] Moreover, if one uses the quantity $T/T_g$ as the reduced temperature, as is the case in the construction of the scaled structural relaxation time (or the scaled viscosity) in the Angell-plot,[40] then a correspondence between the temperature-dependent values of the rate characteristic for different systems will be observed in the vicinity of the glass transition temperature, $T_g$. Consequently, the temperatures $\tilde{T} = T/T_m$ or $\tilde{T} = T/T_g$ cannot be considered to be convenient parameters for the examination of unified regularities, and therefore a more adaptive scaling scheme is required.

In order to compare our results as well as the available experimental data, we apply the method presented in ref. 20. The main idea of this method is to display the temperature dependencies of the quantities in the reduced temperature scale $\tilde{T}$, whereby the values of the zeroth temperature, $T_0 = 0$ K, glass transition temperature, $T_g$, and the melting temperature, $T_m$, are fixed and have the same values of $\tilde{T}_0 = 0$, $\tilde{T}_g = 0.5$ and $\tilde{T}_m = 1$ for all of the systems. The correspondence between the absolute temperatures, $T$, and the reduced temperatures, $\tilde{T}$, is determined by[20]

$$\tilde{T} = K_1\left(\frac{T}{T_g}\right) + K_2\left(\frac{T}{T_g}\right)^2, \tag{18a}$$

with the weight coefficients $K_1$ and $K_2$:

$$K_1 + K_2 = 0.5, \tag{18b}$$

$$K_1 = \left(\frac{0.5 - \frac{T_g^2}{T_m^2}}{1 - \frac{T_g}{T_m}}\right), \quad K_2 = \left(\frac{\frac{T_g}{T_m} - 0.5}{\frac{T_m}{T_g} - 1}\right). \tag{18c}$$

Here, the melting temperature, $T_m$, and the glass transition temperature, $T_g$, are input parameters that are given in absolute units.

Following ref. 20, we assume that the $\tilde{T}$-dependence of the growth rate, $\upsilon_R^{(st)}(\tilde{T})$, and/or $\upsilon_N^{(st)}(\tilde{T})$, obeys the power-law

$$\upsilon_R^{(st)}(\tilde{T}) = \upsilon_R^{(g)}\left(\frac{\tilde{T}}{\tilde{T}_g}\right)^{\chi}, \tag{19}$$

where $\tilde{T}_g = 0.5$ and $\upsilon_R^{(g)}$ is the growth rate of the crystalline nucleus at the temperature, $T_g$. The exponent $\chi > 0$ characterizes the glass-forming properties of the system. Namely, it takes small values for the cases of systems that are not capable of retaining a disordered phase, and, *vice versa*, the exponent $\chi$ must be characterized by high values for good glass-formers.[20] In this regard, it is relevant to mention the recent work of Tang and Harrowell,[14] who demonstrated that the maximum of a crystal growth rate is considered to be a quantity that is correlated with the glass-forming ability. Since the maximum of $\upsilon_R^{(st)}$ is defined by the variation of the growth rate with temperature (with undercooling), then the exponent $\chi$ in eqn (19) can be considered as a simple measure of the glass-forming ability. The validity of eqn (19) is easily tested by mapping the values of the rescaled growth rate onto the logarithmic scale as $(1/\chi)\log_{10}[\upsilon_R^{(st)}(\tilde{T})/\upsilon_R^{(g)}]$. In such a representation, the parameter $\chi$ corrects the slope of the data in the $\tilde{T}$-dependence, and the value of $\chi$ is adjusted so as to map the data onto the master-curve

$$\frac{\upsilon_R^{(st)}(\tilde{T})}{\upsilon_R^{(g)}} = \frac{\tilde{T}}{\tilde{T}_g}. \tag{20}$$

The temperature dependencies of the growth rates evaluated for the cases of the Dz- and bLJ-systems as well as those estimated from molecular dynamics simulations of a crystallized single-component LJ-system[41] and tantal[15] and from the available experimental data for the crystal growth rates, $\upsilon_R^{(st)}$, of $SiO_2$,[42] $PbO{\cdot}SiO_2$,[42] $Li_2O{\cdot}2SiO_2$,[6] $Li_2O{\cdot}3SiO_2$,[43] $CaO{\cdot}MgO{\cdot}2SiO_2$,[44] $2MgO{\cdot}2Al_2O_3{\cdot}5SiO_2$,[44] are presented in Fig. 6. The defined values of the parameter $\chi$ as well as the values of the parameter $\upsilon_R^{(g)}$ for the considered systems are presented in Table 3.

 

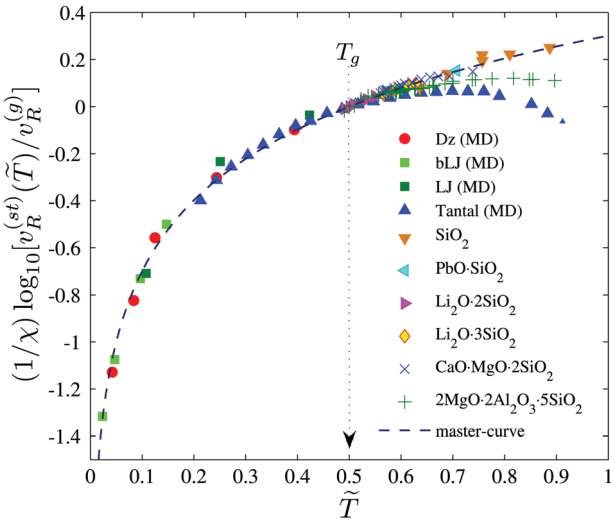


Fig. 6 Scaled growth rates, $v_R^{(st)}$, *vs.* reduced temperature, $\tilde{T}$. Such a plot allows one to compare simulation results for the glassy Dz- and bLJ-systems, simulation results for the supercooled LJ-system[41] and tantal,[15] and the experimental data for supercooled $SiO_2$,[42] $PbO{\cdot}SiO_2$,[42] $Li_2O{\cdot}2SiO_2$,[6] $Li_2O{\cdot}3SiO_2$,[43] $CaO{\cdot}MgO{\cdot}2SiO_2$[44] and $2MgO{\cdot}2Al_2O_3{\cdot}5SiO_2$.[44] The dashed line reproduces the master-curve (20). The arrow indicates the scaled glass transition temperature, $\tilde{T}_g = 0.5$. For the glassy Dz- and bLJ-systems, values of $v_R^{(g)}$ were defined by extrapolation of the data $v_R^{(st)}(\tilde{T})$ to the temperature, $\tilde{T}_g = 0.5$. The values of the parameters $\chi$ and $v_R^{(g)}$ are given in Table 3.

As seen in Fig. 6, the growth rates for all of the systems follow the master-curve (20) for temperatures, $\tilde{T}$, near and below the glass transition temperature, $\tilde{T}_g = 0.5$. The numerical values of the parameters $\chi$ and $v_R^{(g)}$ are given in Table 3. This directly indicates that the behavior of the growth rate $v_R^{(st)}(\tilde{T})$ for the temperature range, $\tilde{T} \leq 0.5$, is reproducible by application of the power-law and that eqn (19) is unified for the $\tilde{T}$-dependent growth rates of the systems. This result is consistent with the findings of ref. 20, in which it was demonstrated that the scaled crystal nucleation time, $\tau_1$, in glassy systems as a function of the reduced temperature, $\tilde{T}$, follows the unified power-law dependence, $\tau_1 \sim (1/\tilde{T})^{\gamma}$. In addition, the power-law temperature dependence of the structural relaxation time, $\tau_\alpha \sim (1/\tilde{T})^{\gamma}$, generalizes the Avramov–Milchev model for the viscosity,[20] while the exponent $\gamma$ is related to the fragility index $m$. Therefore, it is quite reasonable to anticipate that such a temperature dependence is generic for the rate characteristics of structural transformations in glasses, in which the inherent kinetics are dominant over thermodynamic aspects. This differs from how nucleation and growth proceed at low levels of supercooling, where the impact of the thermodynamic contributions on the values of the rates is significant and where the growth rate, $v_R^{(st)}$, increases with increasing supercooling.[3] Thus, the character of the $\tilde{T}$-dependent growth rates for the low supercooling examples diverges from the $\tilde{T}$-dependence specified by eqn (19). As can be seen in Fig. 6, the behavior of the curve $v_R^{(st)}(\tilde{T})$ for the systems starts to become different as the temperature, $\tilde{T}$, approaches the melting point, $\tilde{T}_m = 1$, where the growth rate $v_R^{(st)}(\tilde{T}_m)$ is equal to zero for any system.

### 5.3 Attachment rate

Since the growth kinetics depend directly on the attachment rate, $g_N^+ \equiv g^+(N)$ [see eqn (9)], it is therefore important to consider how the quantity $g_N^+$ behaves with varying temperature, which can be assessed using the term $g_{N_c}^+$, which is the attachment rate for the critically-sized nucleus. We recall here that some theoretical models of growth kinetics (*e.g.* the Turnbull–Fisher model with relation (33) as well as the Kelton–Greer extension with relation (38), see the appendix) utilize the quantity $g_{N_c}^+$ instead of the size dependent $g_N^+$.

The values of the quantity $g_{N_c}^+$ for both of the systems are given in Fig. 7(a), where the temperature is plotted on the reduced scale, $\tilde{T}$. As can be seen, the quantity $g_{N_c}^+$ decreases with decreasing temperature. Nevertheless, the attachment rates as well as the growth rates take finite values for the systems even at deep levels of supercooling, and are still detectable over a simulation time scale. Hence, even insignificant displacements of the particles may result in structural transformations in high-density glassy systems, where the particles interact through an isotropic potential.[20,45,46]

Analogous with the results for the steady-state growth rate (see Fig. 6), the scaled attachment rate *versus* the reduced temperature, $\tilde{T}$, is presented in Fig. 7(b). Here, the parameter $g_{N_c}^{(g)}$ is the attachment rate at the glass transition temperature, $\tilde{T}_g = 0.5$, and its numerical values for the systems are estimated by extrapolation of the attachment rate, $g_{N_c}^+(\tilde{T})$, to the

Table 3 Melting temperature $T_m$, glass transition temperature $T_g$, steady-state growth rate $v_R^{(g)}$ at the transition temperature $T_g$, exponent $\chi$ found from eqn (19), attachment rate $g_{N_c}^{(g)}$ at the glass transition temperature $T_g$, and exponent $\varsigma$ evaluated from fitting eqn (21) to the simulation results

| Ref. | System | $T_m$ | $T_g$ | $v_R^{(g)}$ | $\chi$ | $g_{N_c}^{(g)}$ | $\varsigma$ |
|---|---|---|---|---|---|---|---|
| | Dz (at $P = 14\varepsilon/\sigma^3$) | $1.51\varepsilon/k_B$ | $0.65\varepsilon/k_B$ | $(23.8 \pm 2.7) \times 10^{-4}\sigma/\tau$ | $0.37 \pm 0.06$ | $(13.9 \pm 1.6) \times \tau^{-1}$ | $0.31 \pm 0.04$ |
| | bLJ (at $P = 17\varepsilon/\sigma^3$) | $1.65\varepsilon/k_B$ | $0.92\varepsilon/k_B$ | $(4.7 \pm 0.7) \times 10^{-4}\sigma/\tau$ | $0.41 \pm 0.07$ | $(13.1 \pm 1.5) \times \tau^{-1}$ | $0.58 \pm 0.06$ |
| 41 | LJ | $0.62\varepsilon/k_B$ | $0.4\varepsilon/k_B$ | $0.41 \pm 0.05\sigma/\tau$ | $0.39 \pm 0.07$ | — | — |
| 15 | Ta | 3290 K | 1650 K | $41.5 \pm 4$ m s$^{-1}$ | $3.5 \pm 0.6$ | — | — |
| 42 | $SiO_2$ | 2000 K | 1450 K | $(1.1 \pm 0.2) \times 10^{-12}$ m s$^{-1}$ | $12.6 \pm 1.4$ | — | — |
| 42 | $PbO{\cdot}SiO_2$ | 1037 K | 673 K | $(1.5 \pm 0.2) \times 10^{-11}$ m s$^{-1}$ | $22.6 \pm 1.5$ | — | — |
| 6 | $Li_2O{\cdot}2SiO_2$ | 1306 K | 727 K | $(2.2 \pm 0.4) \times 10^{-12}$ m s$^{-1}$ | $49.2 \pm 4.5$ | — | — |
| 43 | $Li_2O{\cdot}3SiO_2$ | 1306 K | 734 K | $(1.1 \pm 0.3) \times 10^{-11}$ m s$^{-1}$ | $34.5 \pm 2.5$ | — | — |
| 44 | $CaO{\cdot}MgO{\cdot}2SiO_2$ | 1664 K | 993 K | $(9.4 \pm 1.2) \times 10^{-14}$ m s$^{-1}$ | $49.8 \pm 4.8$ | — | — |
| 44 | $2MgO{\cdot}2Al_2O_3{\cdot}5SiO_2$ | 1740 K | 1088 K | $(3.9 \pm 0.8) \times 10^{-12}$ m s$^{-1}$ | $53.2 \pm 6.2$ | — | — |

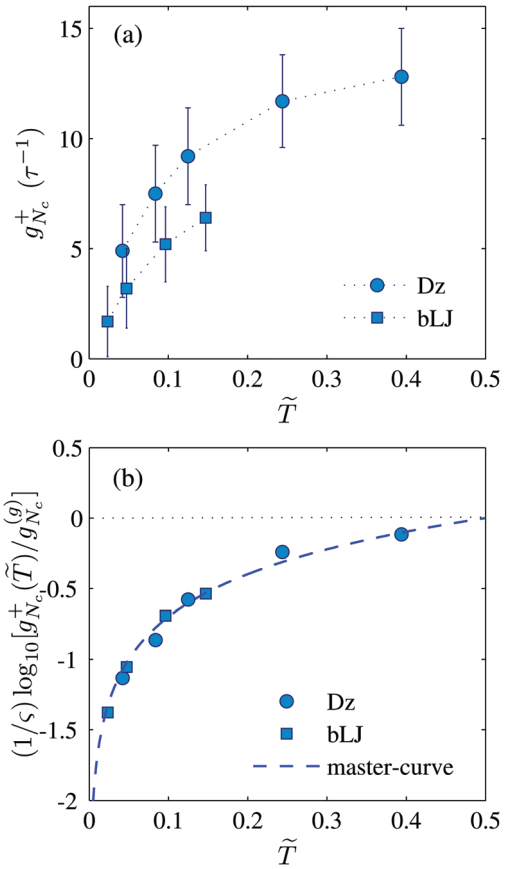


Fig. 7 (a) Attachment rate for the critically-sized nucleus $g^{+}_{N_c}$ as a function of the reduced temperature, $\tilde{T}$, for the Dz-system and bLJ-system. (b) Scaled attachment rate $(1/\varsigma)\log_{10}\left[g^{+}_{N_c}(\tilde{T})\Big/g^{(g)}_{N_c}\right]$ *versus* reduced temperature, $\tilde{T}$. The values of the attachment rate $g^{(g)}_{N_c}$ for the systems are evaluated by extrapolation of the data $g^{+}_{N_c}(\tilde{T})$ to the glass transition temperature $\tilde{T}_g$. The dashed line corresponds to the master-curve, $g^{+}_{N_c}\Big/g^{(g)}_{N_c} = \tilde{T}/\tilde{T}_g$. The values of the exponent $\varsigma$ and the quantity $g^{(g)}_{N_c}$ are given in Table 3.

temperature domain near $\tilde{T}_g$. The exponent $\varsigma$ characterizes how the attachment rate changes with temperature, and is similar to the physical meaning of the exponent $\chi$. When constructing Fig. 7(b), the exponent $\varsigma$ is used as an adjustable parameter that corrects the slope of a curve, while the quantity $g^{(g)}_{N_c}$ is defined in such a way as to guarantee the zeroth value of $(1/\varsigma)\log_{10}\left[g^{+}_{N_c}(\tilde{T})\Big/g^{(g)}_{N_c}\right]$ at the glass transition temperature, $\tilde{T}_g$ = 0.5. The estimated values of the quantities $g^{(g)}_{N_c}$ and $\varsigma$ are given in Table 3. It can be seen in Fig. 7(b) that the $\tilde{T}$-dependencies of the obtained attachment rate, $g^{+}_{N_c}$, for both of the glassy systems are well reproduced by the power-law

$$g^{+}_{N_c}(\tilde{T}) = g^{(g)}_{N_c}\left(\frac{\tilde{T}}{\tilde{T}_g}\right)^{\varsigma}. \qquad (21)$$

[The glass transition temperature is $\tilde{T}_g$ = 0.5].

Remarkably, the exponent $\varsigma$ takes values that are close to the values of the exponent $\chi$ when characterizing the growth kinetics. This is not surprising, since the growth and attachment rates, $\upsilon_N$ and $g^{+}_{N_c}$, are expected to be significantly correlated at deep levels of supercooling. Taking into account the defined values of $g^{(g)}_{N_c}$, we deduce that the attachment rate decreases by two times over the temperature range from $T_g = 0.65\varepsilon/k_B$ to $T = 0.05\varepsilon/k_B$ for the Dz-system and by 4.4 times over the temperature range from $T_g = 0.92/k_B$ to $T = 0.05\varepsilon/k_B$ for the bLJ-system.

## 6 Discussion

Traditional experiments investigating crystal growth are capable of probing crystalline nuclei within the micron size range,[21] and theoretical models of the growth kinetics are required in order to extrapolate the experimental data into the domain of smaller sizes, in which crystal growth initiates, and to obtain an overall picture of the nucleation-growth process (see, for example, ref. 23 and 47). In the current study, we apply an opposite approach. On the basis of the simulation data for model glassy systems at different temperatures, crystal growth is directly restored starting from a nucleation event. This provides us with a possibility to define the time-dependent crystal growth law as well as to evaluate the crystal growth rate characteristics as size- and temperature-dependent terms.

Statistical treatment of the characteristics of the growth kinetics is realized in this study as follows. The growth law is defined by means of the mean-first-passage-time method,[31,33] in which a waiting time scale is set in accordance with a certain size, $N$. As a result, one can estimate the growth laws, $N(t)$, with $N \geq N_c$ on the basis of the independent growth trajectories for the cases when direct averaging, $N(t) = \sum N_\alpha(t)$, does not work, because the nucleation time, $\tau_c$, can take a value from a range that is larger than the characteristic time scale of crystal growth [see Fig. 2(a)]. Within the statistical treatment, the nucleation and growth rate parameters are definable using a common method that utilizes the time-dependent growth trajectories that are obtained from independent experiments or molecular dynamics simulations.

Analysis reveals that the envelope of the nuclei at the initial growth stage is reproduced well by a sphere,[20] while the crystalline faces of the nuclei are not well-defined at this stage.[48] In this case, the average nucleus radius coincides with the proper nucleus radius and one can directly relate the size parameters, the number of particles enclosed in a nucleus, $N$, and the nucleus radius, $R$. This allows one to carry out a reasonable treatment of the results by means of the so-called "mean radius approach".[49] The results obtained in this study reveal that the size of the crystalline nuclei in the considered glassy systems evolves with time at the post-nucleation stage according to dependence, which is an approximate solution of the growth equation. The characteristics of the growth of nascent crystalline nuclei is maintained over the temperature range. As a result, the growth law can be represented in a unified form with the scaled parameters, time, $t/\tau_c$, and size, $N/N_c$. We stress that such characteristics of the growth law are consistent with the limit solution of growth eqn (12), as well as with theoretical suggestions (see p. 378 in ref. 1) and previous simulation results.[20,33,50]

 

The growth rate at the initial growth stage depends strongly on the nucleus size. Nevertheless, at the high levels of supercooling considered in this study, a transition into a steady-state growth regime arises when the nucleus size increases by two-three times with respect to the critical size. Notably, the nucleus size $R$ being equal to $2R_c$ is also mentioned by Langer (p. 14 in ref. 51) and is assumedly related to a maximum of the growth rate, $\upsilon_R$, which arises in the pre-dendridic stage of crystal growth. Hence, crystalline growth in glasses can be characterized by a single value of the growth rate, $\upsilon^{(st)}$, over an extended size range, which simplifies considerably a theoretical description of the crystallization kinetics of the systems.[2,3] Furthermore, according to eqn (12), the size-dependent growth rate, $\upsilon_N$, is defined by three input quantities: the attachment rate, $g^+(N)$, critical size, $N_c$, and reduced difference of the chemical potential, $|\Delta\mu|/k_BT$. Herewith, known theoretical models (see the appendix) are derived from the equation by an approximation for the $N$-dependent attachment rate, $g^+(N)$ (as is done, for example, for the pure kinetic models and for the kinetic extension of the Turnbull–Fisher model, see the appendix) and/or by considering the system under specific thermodynamic conditions with the given ratios of $|\Delta\mu|/k_BT$ and $N_c/N$ (as in the Wilson–Frenkel theory,[52,53] see the appendix). In the present study, a consideration of the growth kinetics was directly carried out on the basis of a primary equation of the growth kinetics, *i.e.* eqn (12).

According to the classical view of the nucleation-growth process,[1] the temperature dependence of the growth rate is characterized by a maximum, which appears due to the features in the $T$-dependence of the kinetic rate coefficient, $g^+(N)$, and the thermodynamic factor (the expression in curly brackets in eqn (9)), for example. Hence, upon decreasing the temperature, the first quantity also decreases, whereas the second term increases. In the current study, we focus on crystalline nuclei growth in glasses at deep levels of supercooling. Under such thermodynamic conditions, the steady-state growth rate, $\upsilon^{(st)}$, is defined mainly by the kinetic term $g^+(N)$ and, therefore, it increases with temperature, $T$, which is opposite to the well-known behavior of the growth rate that is observable experimentally in systems at low and moderate levels of supercooling.[42–44]

General patterns in the temperature dependencies of the growth rate that are detectable for various crystallizing systems[42,44] indicate that a unified theoretical description of the growth rate as a function of temperature as well as a direct comparison of the experimental data for the systems by means of scaling relations are possible. When attempting to carry out such a comparison, one can mention the corresponding part in Langer's review[51] (Fig. 15 on p. 19 and its discussion), in which the growth rates measured for ice and succinonitrile are compared with the Ivantsov relation. In particular, from looking at the results in Fig. 15 given in ref. 51, it follows that the dimensionless growth rate as a function of dimensionless undercooling, which is presented in a double-logarithmic plot, is well interpolated by a power-law dependence. In this work, we extend the idea of a unified description of nucleation-growth kinetics,[40,54,55] which is realized here on the basis of the reduced temperature $\tilde{T}$-scale concept.[20] Note that the reduced temperature $\tilde{T}$-scale differs from the dimensionless temperatures that are usually applied to characterize the thermodynamic states of supercooled liquids and glasses, such as undercooling, $\Delta T/T_m$ (see ref. 56), or dimensionless temperatures, $T/T_m$ and $T/T_g$ (see ref. 40 and 57). Namely, the $\tilde{T}$-scale ranks the temperature range $0 \le T \le T_m$ uniformly for supercooled systems, and, therefore, this allows one to compare the temperature dependent characteristics of the systems, whose glass-forming abilities differ significantly. By means of this approach, we found that the growth rates, extracted from simulations and experimental data for different systems and plotted as a function of $\tilde{T}$ in the temperature range of $0 < T \le T_g$, approximate the power-law dependence on the exponent, which is used as a fitting parameter and which could be used for a numerical estimate of the glass-forming ability of a system.[14] Finally, the attachment rate, which was evaluated on the basis of simulation data and presented as a function of the reduced temperature, $\tilde{T}$, also follows the power-law dependence, which is correlated with the scaling law found before for crystal nucleation times in the systems.[20]

Divergence of the growth rate values and their deviation from the universal power-law at temperatures of $T_g < T < T_m$ is not surprising. At low levels of supercooling, thermodynamic properties have the main impact on the nucleation-growth processes. This is reproducible, in particular, within the Wilson–Frenkel theory (see eqn (27) and (29) in the appendix) and the Turnbull–Fisher model (see eqn (39) in the appendix). Here, the growth rate as well as the nucleation rate increase with increasing supercooling until the system temperature, $T$, is not comparable with the glass transition temperature (*i.e.* $T \le T_g$), at which point the nucleation and growth rates take their highest values. Upon further increasing the supercooling, the slowing down of the system kinetics results in a decrease of all of the transition rate characteristics (namely, the nucleation, growth and attachment rates). Therefore, as is expected, these rates can be correlated as functions of the temperature, $T$, over the range $0 < T \le T_g$. This is supported by the simulation results of this study. Therefore, by taking the reduced chemical potential to be $|\Delta\mu|/(k_BT) \sim 0.19 \pm 0.03$ and the cluster size to be $N \ge 3N_c$, at which point a steady-state growth rate appears for the Dz-system, it is observed that the exponential function in growth eqn (12) becomes approximately equal to unity, whereas $\upsilon_N^{(st)} \sim g_{N_c}^+$ and, consequently, the thermodynamic impact on the growth process is insignificant for the considered temperature range of $0 < T < T_g$.

Finally, the nucleation-growth rate characteristics and, in particular, the kinetic coefficient, $g_{N_c}^+$, are associated with the mobility of particles and, therefore, with diffusion (as it is for $g_{N_c}^+$ in the Kelton–Greer model, for example eqn (34) in the appendix) as well as viscosity (see, for example, the principal equation of the kinetic ballistic model, eqn (41) in the appendix). By making this connection, the unified scenarios in the temperature dependencies of the growth and attachment rates presented in this paper provide new important insight into the possibility of developing a general model of viscosity that is suitable for all supercooled liquids regardless of peculiarities such as fragility, bonding and particle interaction types.[58]

# 7 Conclusions

The main results of this study are the following:

(i) It is shown that the growth law of nuclei of near-critical sizes can be represented as a cubic polynomial with coefficients that are dependent on the critical size, the attachment rate, the chemical potential difference and the growth exponent – *i.e.* all of the quantities that are used in the original growth equation. The growth law model is applied to evaluate the crystal nuclei data derived from molecular dynamics simulations for two different crystallizing glassy systems at temperatures below $T_g$ *via* mean-first-passage-time analysis.

(ii) It is found that the crystal growth laws of the systems follow a unified time-dependence, whereby the growth exponent is constant for each of the systems over the entire considered temperature range.

(iii) The steady-state growth regime, in which the growth rate is independent of the cluster size, occurs when the size of the growing crystalline nucleus in a glassy system becomes two-three times larger than the critical size.

(iv) The results provide evidence that the rate characteristics of the crystal growth process, as temperature dependent quantities, are reproducible within unified scaling relations. This finding is supported for the steady-state growth rate and the attachment rate. The reduced steady-state growth rate values, taken from the simulation results and experimental data for different systems and plotted *vs.* the scaled temperature $\tilde{T}$, collapsed onto a single line at temperatures below $T_g$. In a similar manner, the reduced attachment rates that were evaluated for the crystallizing glassy systems and considered as functions of the reduced temperature, $\tilde{T}$, follow a unified power-law dependence.

# Appendix

### Zeldovich relation

For a metastable system at low levels of supercooling one can consider the dimensionless term

$$\frac{1}{k_B T}\frac{d\Delta G(N)}{dN} \tag{22}$$

as a term that takes small values of less than unity. As a result, eqn (9) simplifies to the well known Zeldovich relation for the growth rate:

$$\upsilon_N = -\frac{g^+(N)}{k_B T}\frac{d\Delta G(N)}{dN}. \tag{23}$$

Zeldovich's relation (23) takes into account the fact that the growth rate is a result of both thermodynamic and pure kinetic contributions, $d\Delta G(N)/dN$ and $g^+(N)$, while their product completely defines the temperature dependence as well as the size dependence of the growth rate. Nevertheless, the aforementioned conditions imposed on the thermodynamic term in eqn (5) restricts the application of the Zeldovich relation (23) to a system under specific thermodynamic conditions.

### Growth rate within the Wilson–Frenkel theory

For a case, when

$$\left(\frac{N_c}{N}\right)^{1/3} \ll 1, \tag{24}$$

that can be realized in the macroscopic limit, *i.e.* at the late stage of growth of a solitary cluster or for a growing crystalline slab, eqn (9) can be rewritten as

$$\upsilon_N = g^+(N)\left\{1 - \exp\left[-\frac{|\Delta\mu|}{k_B T}\right]\right\}. \tag{25}$$

For low and relatively moderate levels of supercooling, *i.e.* for insignificant deviations from equilibrium, the next condition is satisfied:

$$\frac{|\Delta\mu|}{k_B T} \ll 1. \tag{26}$$

Then, eqn (25) takes the form[52,53]

$$\upsilon_N \simeq g^+(N)\frac{|\Delta\mu|}{k_B T}. \tag{27}$$

Taking into account the thermodynamic identity

$$\frac{\Delta\mu}{k_B T} = \frac{l}{T_m}\frac{\Delta T}{k_B T} = \Delta S\frac{\Delta T}{k_B T}, \tag{28}$$

one comes to the known result that the growth rate, $\upsilon_N$, within the Wilson–Frenkel theory[52,53,59] is proportional to supercooling, $\Delta T = T_m - T$. Here, $l$ is the latent heat of the transition and $\Delta S$ is the entropy change between the crystalline and liquid phases. This allows one to rewrite eqn (27) as

$$\upsilon_N = k^{WF}\Delta T, \tag{29}$$

where $k^{WF}$ is the so-called interface kinetic coefficient.

As follows from classical nucleation theory, since the chemical potential difference, $|\Delta\mu|$, is inversely proportional to the critical size, $N_c$ [see eqn (8)], then condition (26) corresponds to large values of the critical size, which indicates the correspondence of eqn (27) to macroscopic growth rates.

### Turnbull–Fisher model and its kinetic extension

The Turnbull–Fisher model was specially adopted to describe crystal nucleation and growth in glasses.[60] The model was extensively studied by Kelton *et al.*[4] and Greer *et al.*[61]

Structural transformations in glasses are driven by kinetic contributions rather than thermodynamic contributions. This means that crystal growth in a glass is largely defined by diffusive processes. In this model it is assumed that the coefficient $g^+(N)$ can be taken in the form

$$g^+(N) \sim \exp\left[-\frac{\Delta G(N+1) - \Delta G(N)}{2k_B T}\right]. \tag{30}$$

 

Inserting eqn (30) into eqn (4), by analogy with eqn (5), one obtains

$$\upsilon_N \sim \exp\left[-\frac{1}{2k_BT}\frac{d\Delta G(N)}{dN}\right] - \exp\left[\frac{1}{2k_BT}\frac{d\Delta G(N)}{dN}\right] \sim 2\sinh\left[-\frac{1}{2k_BT}\frac{d\Delta G(N)}{dN}\right]. \quad (31)$$

Then, taking into account eqn (7), one obtains the growth rate

$$\upsilon_N \sim 2\sin h\left\{\frac{|\Delta\mu|}{2k_BT}\left[1-\left(\frac{N_c}{N}\right)^{1/3}\right]\right\}. \quad (32)$$

As a result, the expression for the Turnbull–Fisher cluster-size-dependent growth rate can be written as

$$\upsilon_N = 2g^+(N_c)\left(\frac{N}{N_c}\right)^{2/3} \times \sin h\left\{\frac{|\Delta\mu|}{2k_BT}\left[1-\left(\frac{N_c}{N}\right)^{1/3}\right]\right\}, \quad (33)$$

The Turnbull–Fisher model was later extended by Kelton and Greer,[62] who expressed the coefficient, $g^+(N_c) \equiv g^+_{N_c}$, in terms of the ordinary diffusion, $D$, as

$$g^+(N_c) = 24\frac{D}{\lambda^2}N_c^{2/3}, \quad (34)$$

where $\lambda$ is the atomic jump distance. As a result, eqn (33) takes the form

$$\upsilon_N = 48\frac{D}{\lambda^2}N^{2/3}\sinh\left\{\frac{|\Delta\mu|}{2k_BT}\left[1-\left(\frac{N_c}{N}\right)^{1/3}\right]\right\}. \quad (35)$$

For growth under macroscopic conditions, when the size of the growing cluster is much larger than the critical size, $N_c$, eqn (33) and (35) take the forms,

$$\upsilon_N = 2g^+(N_c)\left(\frac{N}{N_c}\right)^{2/3}\sinh\left\{\frac{|\Delta\mu|}{2k_BT}\right\} \quad (36)$$

and

$$\upsilon_N = 48\frac{D}{\lambda^2}N^{2/3}\sinh\left\{\frac{|\Delta\mu|}{2k_BT}\right\} \quad (37)$$

respectively.

It is easy to verify that, at low levels of supercooling, eqn (36) and (37) are simplified to the following corresponding relations

$$\upsilon_N = g^+(N_c)\left(\frac{N}{N_c}\right)^{2/3}\frac{|\Delta\mu|}{k_BT} \quad (38)$$

and

$$\upsilon_N = 24\frac{D}{\lambda^2}N^{2/3}\frac{|\Delta\mu|}{k_BT}. \quad (39)$$

In eqn (38) and (39), the contribution responsible for reproducing the thermodynamic aspect of cluster growth remains the same, since the Kelton–Greer extension concerns only the kinetic contribution of the Turnbull–Fisher model.

Furthermore, by taking into account equality (28), one can see that eqn (38) and (39) yield the same linear dependence of the macroscopic growth rate upon the supercooling, *i.e.* $\upsilon_N \propto \Delta T$,

$$\upsilon_N \propto \frac{|\Delta\mu|}{k_BT} \propto \frac{l}{T_m}\frac{\Delta T}{k_BT} \propto \Delta S\frac{\Delta T}{k_BT}, \quad (40)$$

which is the same with eqn (29) which is derived from the Wilson–Frenkel theory.

### Kinetic models

There are some pure kinetic growth models that are rather focused upon the mechanisms of mass exchange between the cluster and the mother phase.[23] Hence, the $N^{2/3}$-dependence for the coefficient $g^+(N)$ is suggested in the so-called ballistic model[63]

$$g^+(N) = b\frac{k_BT}{\eta\lambda^3}N^{2/3}, \quad (41)$$

where $\eta$ is the viscosity, and $b$ is a numerical constant. Since, for three-dimensional growth, one has $dR/dt \propto N^{-2/3}dN/dt$, then the ballistic model with eqn (41) corresponds to the rate, $g^+(N)$, which is actually independent of the radius of the cluster, but depends on the properties of the mother phase. As was discussed in ref. 63, such a scenario is appropriate, in particular, for the case of fluid droplet growth in a supersaturated vapor.

Furthermore, in the growth kinetics of Ostwald ripening regimes, other situations appear,[26,64,65] where the rate, $g^+(N)$, exhibits size-dependence in the form

$$g^+(N) \propto N^{1/3} \quad (42a)$$

and the rate, $g^+(N)$, can even be independent of the size

$$g^+(N) = \text{const.} \quad (42b)$$

As can be seen, relations (41), (42a) and (42b) can be generalized into the power-law dependence[21,23]

$$g^+(N) \propto N^{(3-p)/3}, \quad (43)$$

with $0 < p \leq 3$, where the integer values of the exponent, *i.e.* $p = 1, 2, 3$, correspond to the models (41), (42a) and (42b), respectively.

## Acknowledgements

The authors thank E. Zanotto, D. Kashchiev, V. N. Ryzhov and V. V. Brazhkin for motivating discussions. The work is supported in part by the grant MD-5792.2016.2 (support for young scientists in RF) and by the project of state assignment of KFU in the sphere of scientific activities.

## References


1 D. Kashchiev, *Nucleation: Basic Theory with Applications*, Butterworth Heinemann, Oxford, UK, 2000.
2 V. P. Skripov, *Metastable Liquids*, Wiley, New-York, 1974.
3 P. G. Debenedetti, *Metastable Liquids. Concepts and Principles*, Princeton U.P., Princeton, 1996.
4 K. F. Kelton, A. L. Greer and C. B. Thompson, *J. Chem. Phys.*, 1983, **79**, 6261–6276.
5 V. I. Kalikmanov, *Nucleation Theory*, Lecture Notes in Physics, Springer, New York, 2012.
6 V. M. Fokin, N. S. Yuritsin, O. V. Potapov, B. S. Shakhmatkin, N. M. Vedisheva, V. L. Ugolkov and A. G. Cherepova, *Russ. J. Phys. Chem. A*, 2003, **77**, 146.
7 L. Yang, L. JiaHao and L. BaiXin, *Phys. Chem. Chem. Phys.*, 2015, **17**, 27127–27135.
8 H. W. Choi, Y. H. Kim, Y. H. Rimc and Y. S. Yang, *Phys. Chem. Chem. Phys.*, 2013, **15**, 9940–9946.
9 E. Amstad, F. Spaepena and D. A. Weitz, *Phys. Chem. Chem. Phys.*, 2015, **17**, 30158–30161.
10 N. Bosq, N. Guigo, J. Persello and N. Sbirrazzuoli, *Phys. Chem. Chem. Phys.*, 2014, **16**, 7830–7840.
11 S. Liang, D. Rozmanov and P. G. Kusalik, *Phys. Chem. Chem. Phys.*, 2011, **13**, 19856–19864.
12 E. B. Moore and V. Molinero, *Phys. Chem. Chem. Phys.*, 2011, **13**, 20008–20016.
13 P. Rein, ten Wolde and D. Frenkel, *Phys. Chem. Chem. Phys.*, 1999, **1**, 2191–2196.
14 C. Tang and P. Harrowell, *Nat. Mater.*, 2013, **12**, 507–511.
15 L. Zhong, J. Wang, H. Sheng, Z. Zhang and S. X. Mao, *Nature*, 2014, **512**, 177–180.
16 J. A. D. Wattis and P. V. Coveney, *Phys. Chem. Chem. Phys.*, 1999, **1**, 2163–2176.
17 M. C. Wilding, M. Wilson, P. F. McMillan, T. Deschampsd and B. Champagnon, *Phys. Chem. Chem. Phys.*, 2014, **16**, 22083–22096.
18 C. A. Lemarchand, *J. Chem. Phys.*, 2012, **136**, 234505.
19 C. A. Lemarchand, *J. Chem. Phys.*, 2013, **138**, 034506.
20 A. V. Mokshin and B. N. Galimzyanov, *J. Chem. Phys.*, 2015, **142**, 104502.
21 M. C. Weinberg, W. H. Poisl and L. Granasy, *C. R. Chim.*, 2002, **5**, 765–771.
22 Ya. B. Zeldovich, *Acta Physicochim. URSS*, 1943, **18**, 1–92.
23 V. A. Shneidman and M. C. Weinberg, *J. Chem. Phys.*, 1992, **97**, 3621–3628.
24 S. A. Kukushkin and A. V. Osipov, *J. Exp. Theor. Phys.*, 1998, **86**, 1201–1208.
25 F. Liu, F. Sommer, C. Bos and E. J. Mittemeijer, *Int. Mater. Rev.*, 2007, **52**, 193–212.
26 S. A. Kukushkin and A. V. Osipov, *Prog. Surf. Sci.*, 1996, **51**, 1–107.
27 M. Dzugutov, *Phys. Rev. Lett.*, 1993, **70**, 2924–2927.
28 J. Roth and A. R. Denton, *Phys. Rev. E: Stat. Phys., Plasmas, Fluids, Relat. Interdiscip. Top.*, 2000, **61**, 6845–6857.
29 P. R. ten Wolde, M. J. Ruiz-Montero and D. Frenkel, *J. Chem. Phys.*, 1996, **104**, 9932–9947.
30 P. J. Steinhardt, D. R. Nelson and M. Ronchetti, *Phys. Rev. B: Condens. Matter Mater. Phys.*, 1983, **28**, 784–805.
31 A. V. Mokshin and B. N. Galimzyanov, *J. Chem. Phys.*, 2014, **140**, 024104.
32 P. Hänggi, P. Talkner and M. Borkovec, *Rev. Mod. Phys.*, 1990, **62**, 251–340.
33 A. V. Mokshin and B. N. Galimzyanov, *J. Phys. Chem. B*, 2012, **116**, 11959–11967.
34 A. V. Mokshin, B. N. Galimzyanov and J.-L. Barrat, *Phys. Rev. E: Stat., Nonlinear, Soft Matter Phys.*, 2013, **87**, 062307.
35 A. V. Mokshin and J.-L. Barrat, *Phys. Rev. E: Stat., Nonlinear, Soft Matter Phys.*, 2008, **77**, 021505.
36 A. V. Mokshin and J.-L. Barrat, *J. Chem. Phys.*, 2009, **130**, 034502.
37 A. V. Mokshin and J.-L. Barrat, *Phys. Rev. E: Stat., Nonlinear, Soft Matter Phys.*, 2010, **82**, 021505.
38 C. Valeriani, E. Sanz and D. Frenkel, *J. Chem. Phys.*, 2005, **122**, 194501.
39 M. Mosayebi, E. D. Gado, P. Ilg and H. C. Öttinger, *J. Chem. Phys.*, 2012, **137**, 024504.
40 C. A. Angell, *Science*, 1995, **267**, 1924–1935.
41 J. Q. Broughton, G. H. Gilmer and K. A. Jackson, *Phys. Rev. Lett.*, 1982, **49**, 1496–1500.
42 M. L. F. Nascimento and E. D. Zanotto, *J. Chem. Phys.*, 2010, **133**, 174701.
43 T. Ogura, R. Hayami and M. Kadota, *J. Ceram. Assoc. Jpn.*, 1968, **76**, 277–284.
44 S. Reinsch, M. L. F. Nascimento, R. Muller and E. D. Zanotto, *J. Non-Cryst. Solids*, 2008, **354**, 5386–5394.
45 R. M. Khusnutdinoff and A. V. Mokshin, *Phys. A*, 2012, **391**, 2842–2847.
46 R. M. Khusnutdinoff and A. V. Mokshin, *J. Non-Cryst. Solids*, 2011, **357**, 1677–1684.
47 L. Gránásy and P. F. James, *J. Chem. Phys.*, 2000, **113**, 9810–9821.
48 K. F. Kelton, *Solid State Phys.*, 1991, **45**, 75–177.
49 M. Perez, M. Dumont and D. Acevedo-Reyes, *Acta Mater.*, 2008, **56**, 2119–2132.
50 A. V. Mokshin and B. N. Galimzyanov, *J. Phys.: Conf. Ser.*, 2012, **394**, 012023.
51 J. S. Langer, *Rev. Mod. Phys.*, 1980, **52**, 1–28.
52 H. A. Wilson, *Philos. Mag.*, 1900, **50**, 238–250.
53 J. Frenkel, *Phys. Z. Sowjetunion*, 1932, **1**, 498–500.
54 B. N. Hale, *Phys. Rev. A: At., Mol., Opt. Phys.*, 1986, **33**, 4156–4163.
55 B. N. Hale and M. Thomason, *Phys. Rev. Lett.*, 2010, **105**, 046101.
56 J. Frenkel, *Kinetic Theory of Liquids*, Oxford University Press, London, 1946.
57 C. A. Angell, C. A. Scamehorn, D. J. List and J. Kieffer, *Proceedings of XV International Congress on Glass*, Leningrad, 1989.
58 M. E. Blodgett, T. Egami, Z. Nussinov and K. F. Kelton, *Sci. Rep.*, 2015, **5**, 13837.
59 A. Kerrache, J. Horbach and K. Binder, *EPL*, 2008, **81**, 58001.


 

60 D. Turnbull and J. C. Fisher, *J. Chem. Phys.*, 1949, **17**, 71–73.
61 A. L. Greer, P. Y. Evans, R. G. Hamerton, D. K. Shanagguan and K. F. Kelton, *J. Cryst. Growth*, 1990, **99**, 38–45.
62 K. F. Kelton and A. L. Greer, *J. Non-Cryst. Solids*, 1986, **79**, 295–309.
63 V. Volterra and A. R. Cooper, *J. Non-Cryst. Solids*, 1985, **74**, 85–95.
64 J. S. Langer and A. J. Schwartz, *Phys. Rev. A: At., Mol., Opt. Phys.*, 1980, **21**, 948–958.
65 G. T. Rengarajan, D. Enke, M. Steinharta and M. Beiner, *Phys. Chem. Chem. Phys.*, 2011, **13**, 21367–21374.